Gamow-Teller strength to ^{38}K from the ^{38}Ar(p,n) reaction and ^{38}Ca(β^+) decay

B. D. Anderson,[1] A. R. Baldwin,[1] P. Baumann,[2] B. A. Brown,[3] F. Didierjean,[2,*] C. C. Foster,[4] L. A. C. Garcia,[1,†]
A. Huck,[2] A. Knipper,[2] R. Madey,[1,5] D. M. Manley,[1] G. Marguier,[6] M. Ramdhane,[2,‡] H. Ravn,[7] C. Richard-Serre,[8]
G. Walter,[2] and J. W. Watson[1]

[1]*Department of Physics and Center for Nuclear Research, Kent State University, Kent, Ohio 44242*
[2]*Centre de Recherches Nucléaires, Université Louis Pasteur, Strasbourg, France and the ISOLDE Collaboration*
[3]*National Superconducting Cyclotron Laboratory and Department of Physics, Michigan State University, East Lansing, Michigan 48824*
[4]*Indiana University Cyclotron Facility, Bloomington, Indiana 47408*
[5]*Department of Physics, Hampton University, Hampton, Virginia 23668*
[6]*Institut de Physique Nucléaire, Université Claude Bernard, Villeurbanne, France and the ISOLDE Collaboration*
[7]*ISOLDE Collaboration, CERN, Geneva, Switzerland*
[8]*ISOLDE Collaboration, CERN and IN2P3, Geneva, Switzerland*

(Received 28 March 1996)

Gamow-Teller (1^+) strength was studied in ^{38}K with the analog reactions ^{38}Ar(p,n)^{38}K and ^{38}Ca(β^+)^{38}K. The (p,n) reaction was performed at 135 MeV using the beam swinger facility at the Indiana University Cyclotron Facility. Excitation-energy spectra were measured at 15 angles between 0° and 63°. Neutron energies were measured by the time-of-flight method using a large-volume plastic scintillator array at a flight path of 131.0 m. The overall energy resolution was 280 keV. Gamow-Teller (GT) strength was extracted from the measured angular distributions to discrete 1^+ final states. The β-decay experiment was performed with the ISOLDE on-line mass separator facility at CERN. The β-decay branching ratios were determined by observing the delayed γ decays of ^{38}K. These decay measurements provide an increased sensitivity over earlier measurements and are able to extract transitions down to $\sim 10^{-4}$ of the strongest branches. The B(GT) values obtained from the two experiments are generally in good agreement, except for the transition to the first 1^+ state at 0.46 MeV, which is observed to be much weaker in the (p,n) measurements. The β-decay measurements provide good resolution and high sensitivity while the (p,n) measurements extend the β-decay measurements to higher excitation energies. The summed B(GT) strength is $\sim$50% of the simple Ikeda sum rule. The distribution of GT strength is in reasonable agreement with that predicted from a shell-model calculation using ''effective'' GT operators. [S0556-2813(96)05608-7]

PACS number(s): 25.40.Kv, 23.40.Hc, 21.60.Cs, 27.30.+t

I. INTRODUCTION

The study of Gamow-Teller (GT) strength in nuclei continues to be a topic of high interest. GT transitions correspond to a particularly simple process that should be amenable to accurate theoretical description. These transitions involve spin and isospin transfer, and the mapping of such strength in a nucleus provides an important test of structure calculations for that nucleus. The special interest in studies of GT strength arises from the fact that such strength in both light and heavy nuclei is generally ''quenched'' from that expected using ''free-nucleon'' GT operators (i.e., obtained from the β decay of the free neutron) and structure wave functions obtained from the nuclear shell model. This quenching is seen in β-decay strengths [1,2] and also in (p,n)[3–5], (p,p')[6,7], and (e,e') [8] reaction studies. The existence of such quenching presents a significant problem and various mechanisms have been proposed to explain this quenching, including coupling to Δ-hole excitations, iso-

bar diagrams, and higher-order multiparticle-multihole configurational mixing. The basic question is whether the quenching can be explained in terms of the nuclear structure involved or whether the GT operator is significantly altered in the presence of nuclear matter. This quenching is often discussed in relationship with the model-independent sum rule of Ikeda [9]:

$$B(\mathrm{GT}_-) - B(\mathrm{GT}_+) = \sum_f \langle f|\sigma t_-|i\rangle^2 - \sum_f \langle f|\sigma t_+|i\rangle^2$$
$$= 3(N_i - Z_i).$$

In this expression, σ is the Pauli spin operator, $t_\pm$ are the isospin raising and lower operators, and $|i\rangle$ and $\langle f|$ are the initial and final nuclear wave functions.

In an analysis of ^{37}Ca β-decay data, Adelberger *et al.* [10] questioned the extent to which the weak GT operator is renormalized in nuclei [11]. They noted that the GT decay strength extracted from these data was about equal to that obtained from a shell-model calculation together with the free-nucleon value for the GT operator; and they indicated that this cast some doubt on previous conclusions that the experimental GT strength for nuclei with $A = 17–39$ was systematically quenched to only about 60% of that expected from $1s0d$ shell-model calculations. The shell-model calcu-

---

*Present address: Eurisys Mesures, 67380 Lingolsheim, France.

†Present address: Physics Department, Southern University, Baton Rouge, LA 70813.

‡Permanent address: Ecole Normale Supérieure Oum-El-Bouagui, University of Constantine, Algeria.

lations were performed using the "universal" $1s0d$ (USD) matrix elements of Wildenthal [2]. Later, Brown [12] showed that the quenching extracted from the ^{37}Ca β-decay data is more model dependent than most previous analyses of GT data and that, if one uses the Chung-Wildenthal Hamiltonian (CWH), one can reproduce the shape of the observed β-decay strength. The predictions obtained using the CWH interaction are about two times larger than the experimental results, so that the quenching inferred is then about the same as that obtained from the global analysis of all $1s0d$-shell β-decay data. More recently, Trinder *et al.* [13] studied GT strength in the β decay of ^{36}Ca. They found that the weak GT strength to the low-lying levels (below 5 MeV) is better reproduced by the USD interaction but, as in the ^{37}Ca decay, the strength to the higher levels at 6–8 MeV is reproduced better with the CWH interaction. It appears that the ideal interaction is some combination of USD and CWH. For both ^{37}Ca and ^{36}Ca, the total strength is the same with the USD and CWH interactions, but the CWH GT strength is shifted down in energy relative to USD, leading to better agreement with the experiment at low and medium excitation energies. Also for both ^{37}Ca and ^{36}Ca, the "giant" GT resonance strength is predicted to lie above the β-decay Q-value window.

In this paper, we present new (p,n) data for the neighboring nucleus ^{38}Ar along with new data for the analog β decay, ^{38}Ca$(\beta^+)^{38}$K. This case is close to that for ^{37}Ca (and is in the upper part of the $1s0d$ shell); furthermore, for the comparison between the hadronic and weak probes, it has the advantage that it involves an even-A nucleus. It is known that GT transitions in (p,n) reactions involving odd-A nuclei often show marked deviation from the "universal" conversion factor for comparing $0°$ (p,n) cross sections with B(GT) values obtained in analog β decays observed for even-A nuclei [14]. The sources of these deviations are not understood and have been ascribed to both structure and reaction-mechanism effects. Some cases, viz., $A=13$, 15, and 39 show deviations of nearly a factor of 2 from the general trend; in contrast, strong GT transitions in even-A nuclei seem to agree with this universal conversion factor to within $\pm 15\%$. Additionally, for ^{38}Ar$(p,n)^{38}$K, the conversion to B(GT) values can be checked for several transitions against the measured analog β decay, ^{38}Ca$(\beta^+)^{38}$K, since the β-decay Q-value window allows one to observe transitions up to higher energies in the residual nucleus than usual (viz., up to 6.7 MeV). To probe accurately the GT strength in the full Q_β energy range, it is necessary to measure β branches in the ^{38}Ca decay down to the 10^{-4} level. Therefore the present study was undertaken to reach a new level of sensitivity and make possible a good comparison between the results of β-decay and of the isospin analog (p,n) reaction within the experimental window. Although in this specific case, most of the predicted GT strength lies within the range accessible to both probes, it is important to see what GT strength exists above the β-decay "window" and this can be done with the (p,n) reaction. In this work, the (p,n) and the β-decay results are compared also with theoretical calculations based on the CWH interaction, which was used by Brown for the $A=36$ and 37 analyses [12,13].

II. THE ^{38}Ar$(p,n)^{38}$K REACTION

A. Experimental procedure

The (p,n) experiment was performed at the Indiana University Cyclotron Facility (IUCF) with the beam-swinger system. The experimental arrangement and data reduction procedures were similar to those described previously [15,16]. Neutron kinetic energies were measured by the time-of-flight (TOF) technique. A beam of 135-MeV protons was obtained from the cyclotron in narrow beam bursts typically 350 ps long, separated by ~ 2 μs. The long time between beam bursts was obtained by use of a small storage ring between the beam source and the main cyclotron, referred to as the "stripper loop." This long time between beam bursts eliminates "overlap" background from previous beam bursts and greatly reduces the cosmic-ray background as well. Neutrons were detected in three detector stations at $0°$, $24°$, and $45°$ with respect to the undeflected proton beam. The flight paths were 131.0, 130.2, and 81.4 m (± 0.2 m), respectively. The neutron detectors were rectangular bars of fast plastic scintillator, 10.2-cm thick. Three separate detectors, each 1.02 m long by 0.51 m high, were combined for a total frontal area of 1.55 m^2 in the $0°$ and $24°$ stations. The $45°$ station had two detectors, each 1.52 m long by 0.76 m high, for a total frontal area of 2.31 m^2. Each neutron detector had tapered Plexiglass light pipes attached on the two ends of the scintillator bar, coupled to 12.8-cm diam phototubes. Timing signals were derived from each end and combined in a mean-timer circuit [17] to provide the timing signal from each detector. Overall time resolutions of about 825 ps were obtained, including contributions from the beam burst width (≈ 350 ps), beam-energy spread (≈ 400 ps), energy loss in the target (≈ 300 ps), neutron transit times across the 10.2-cm thickness of the detectors (≈ 530 ps), and the intrinsic time dispersion of each detector (≈ 300 ps). This overall time resolution provided an energy resolution of about 280 keV in the first two detector stations and about 450 keV in the widest-angle station. The large-volume detectors were described in more detail previously [18]. Protons from the target were rejected by anticoincidence detectors in front of each neutron detector array. Cosmic rays were vetoed by anticoincidence detectors on top of each array as well as the ones at the front.

The target was a low-volume cylindrical gas cell 4 cm long by 1 cm diameter. The entrance and exit windows were 25.4-μm Kapton. The cell was filled to ~ 2 atm absolute with ^{38}Ar gas, enriched to 95%. Empty-cell runs were performed to subtract contributions from the Kapton windows. Time-of-flight spectra were obtained at 15 angles between $0°$ and $63°$. Spectra from each detector were recorded at ten pulse-height thresholds from 5 to 50 MeV equivalent-electron energy (MeVee). Calibration of the pulse-height response of each of the detectors was performed with a ^{228}Th source ($E_\gamma = 2.61$ MeV) and a calibrated fast amplifier. The values of the cross sections extracted for different thresholds were found to be the same within statistics. The values of the cross sections reported here are at a threshold setting of 10 MeVee.

B. Data reduction

Excitation-energy spectra were obtained from the measured TOF spectra using the known flight paths and a cali-

bration of the time-to-amplitude converter. Strong transitions to known states in the residual nucleus ^{38}K as well as the strong ^{12}C(p,n)^{12}N(g.s.) transition from the ^{12}C in the Kapton windows provided absolute reference points. Absolute neutron kinetic energies (and therefore excitation energies) are estimated to be accurate to ± 0.1 MeV. Yields for individual transitions were obtained by peak fitting of the TOF spectra.

In order to obtain excitation-energy spectra for the ^{38}Ar(p,n)^{38}K reaction, it was necessary to subtract the contributions from the Kapton entrance and exit windows of the gas cell. This was performed in the TOF spectra by subtracting empty-cell runs. The TOF spectra were aligned using the strong ^{12}C(p,n)^{12}N peaks. The empty-cell run was normalized to the full-cell run by comparing yields in the ^{12}C(p,n) peaks. Because there is additional energy loss in the ^{38}Ar gas for a full-cell run, the peaks in an empty-cell run were somewhat narrower than for a full-cell run. This difference produced positive and negative swinging oscillations for subtraction of peaks, even when properly normalized. We eliminated this problem to first order by performing a Gaussian smearing of the empty-cell runs to broaden the TOF peaks. Because of the difference in reaction Q values, these subtraction problems appear only above $E_x = 11$ MeV, and are not a problem for the primary region of interest in this work.

Yields for transitions in the ^{38}Ar(p,n)^{38}K reaction were obtained by peak fitting of the TOF spectra. The spectra were fitted with an improved version of the peak-fitting code of Bevington [19]. Examples of similar peak fitting of (p,n) neutron TOF spectra were presented previously [15,16]. The minimum number of peaks required to fit the data were used, consistent with the requirement that the fits proceed smoothly from one angle to the next. Widths for small peaks were constrained to be the same as that observed for the largest peak in the region. Cross sections were obtained by combining the yields with the measured geometrical parameters, the beam integration, and the target thickness. The neutron efficiencies were obtained from a Monte Carlo computer code [20], which was tested at these energies [21,22]. The experimental procedure and data reduction were similar to those described in more detail in Refs. [15,16]. The uncertainty in the overall scale factor is dominated by the uncertainty in the detector efficiencies and is estimated to be $\pm 12\%$. The uncertainties shown in the angular distributions (see below) are only from the fitting uncertainties.

C. Results and discussion

The excitation-energy spectrum for the ^{38}Ar(p,n)^{38}K reaction at 135 MeV and 0° is shown in Fig. 1. Angular distributions were extracted for all peaks observed in this spectrum. These angular distributions are shown in Figs. 2 and 3. Some of these peaks correspond to complexes of more than one state and are discussed more fully below. No peaks are observed above 10.5 MeV at forward angles, where one expects GT transitions to appear. In the following sections we discuss each of these excitations separately. Each angular distribution is compared with a distorted-wave impulse-approximation (DWIA) calculation. These calculations were performed using the code DW81 [23] with the nucleon-
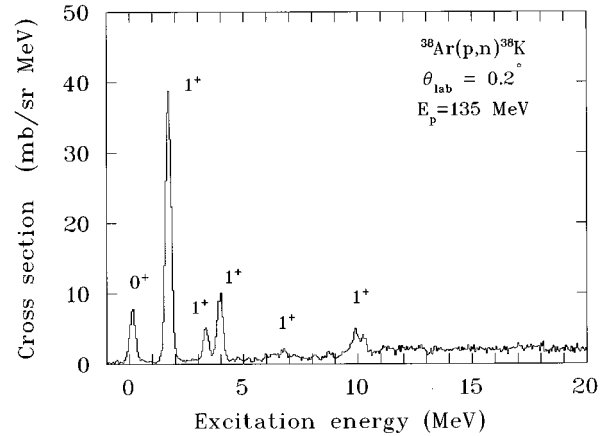

FIG. 1. Excitation-energy spectrum for the ^{38}Ar(p,n)^{38}K reaction at 135 MeV and 0°.

nucleon effective interaction of Franey and Love at 140 MeV [24] and optical-model wave functions obtained from the global parameter set of Schwandt *et al.* [25]. The nuclear wave functions were calculated using the shell-model code OXBASH [26] with the basis taken to be the full $0s1d$ shell (unrestricted) and the modified Chung-Wildenthal Hamiltonian (CWH) interaction as described by Brown [12].

D. The complex at 0.1–0.4 MeV

The first three levels of ^{38}K appear unresolved in this experiment and are known to be the 3^+ ground state, a 0^+ state at 0.13 MeV, and a 1^+ state at 0.46 MeV. By peak fitting, using peak widths corresponding to the known resolution (observed for other peaks), we are able to separate the 1^+ state at 0.46 MeV from the other two levels. Examples of the fitting for this complex at 0° and 11.5° are shown in Fig. 4. The angular distributions for these two peaks are shown in Fig. 2. The angular distribution for the 3^+, 0^+ doublet at 0.0 and 0.13 MeV, respectively, is fitted fairly well by the combined DWIA calculations for these two transitions. The final-state wave functions are for the first 0^+ and 3^+ states in the shell-model calculations described above. The 0^+ DWIA calculation is a ''density-dependent'' calculation; it was found earlier that such calculations are necessary for accurate descriptions of 0^+ to 0^+ IAS transitions, which are sensitive to Pauli-blocking effects [27]. We see that the forward peak in this angular distribution is described fairly well by such a calculation with a normalization factor slightly greater than unity. This calculation does not account for the second maximum near 35°, which, however, is described well by the 3^+ calculation with a normalization factor of 0.13, indicating that this transition is probably affected strongly by correlations outside the basis assumed for the shell-model calculations.

The angular distribution for the 1^+ state at 0.46 MeV is not peaked at 0° and is, in fact, quite weak (cf., the other 1^+ excitations described below). Although this transition is weak and not cleanly resolved in the (p,n) measurements, we believe that we were able to extract the strength reliably with an uncertainty of $\pm 50\%$ or less. The data and fits at 0° and 12° shown in Fig. 4 show a definite shoulder at 12° from the transition to the 0.46-MeV state; at 0°, this contri-
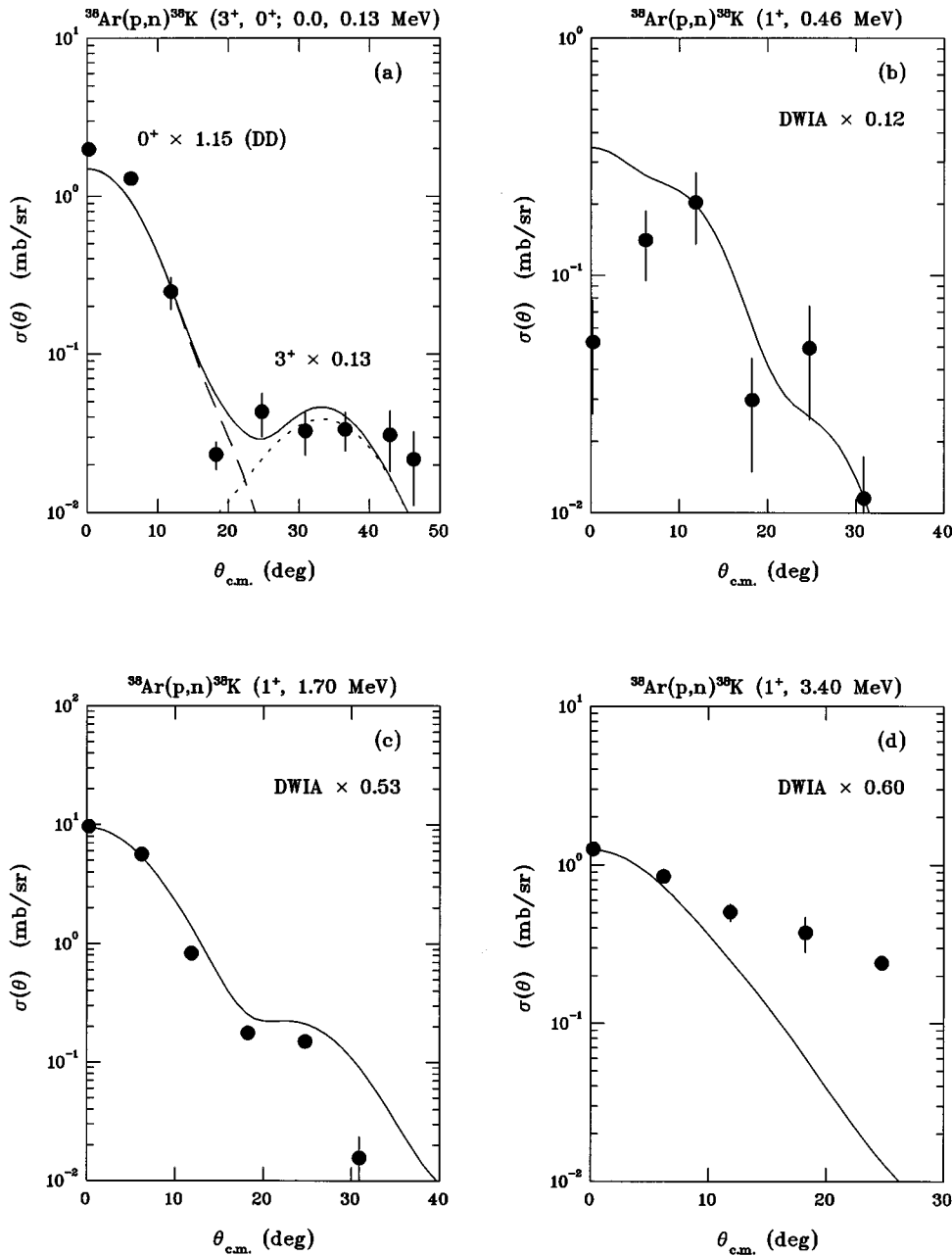
FIG. 2. Angular distributions for the ^{38}Ar$(p,n)^{38}$K reaction at 135 MeV to the final states at 0.13, 0.46, 1.7, and 3.4 MeV.

bution is clearly weaker. This transition appears to be "ℓ forbidden" and is described poorly by the DWIA calculation for the first 1^+ state. This transition is discussed further below.

1. The 1^+ state at 1.7 MeV

The strongest excitation seen in Fig. 1 is to the known 1^+ state at 1.698 MeV. This transition carries more than one-half of all the 1^+ strength observed in this reaction. The angular distribution is presented in Fig. 2 and is described quite well by the DWIA calculation for the second 1^+ state with a normalization factor of 0.53. This normalization factor is typical for strong 1^+ transitions in the $1s0d$ shell and is an indication of "quenching" of GT strength in this reaction.

2. The 1^+ states at 3.4 and 3.9 MeV

The next peaks observed in the 0.2° spectrum of Fig. 1 are at 3.4 and 3.9 MeV. The angular distributions for these two peaks are presented in Figs. 2 and 3. These peaks correspond fairly well with two 1^+ states reported previously at 3.3 and 3.4 MeV, and four 1^+ states reported between 3.7 and 4.0 MeV [28]. The shell-model calculations predict one peak in this region at 3.9 MeV and the DWIA calculations shown use the wave function for this state. The 3.9-MeV transition is fitted well with a normalization factor of 1.20. The 3.4-MeV transition shows additional experimental strength at wider angles, indicating that this complex probably includes some states with higher spins. The level density of states at this excitation energy is such that this is likely. The DWIA normalization factor required to make the DWIA calculation agree with the data at 0° is 0.60.

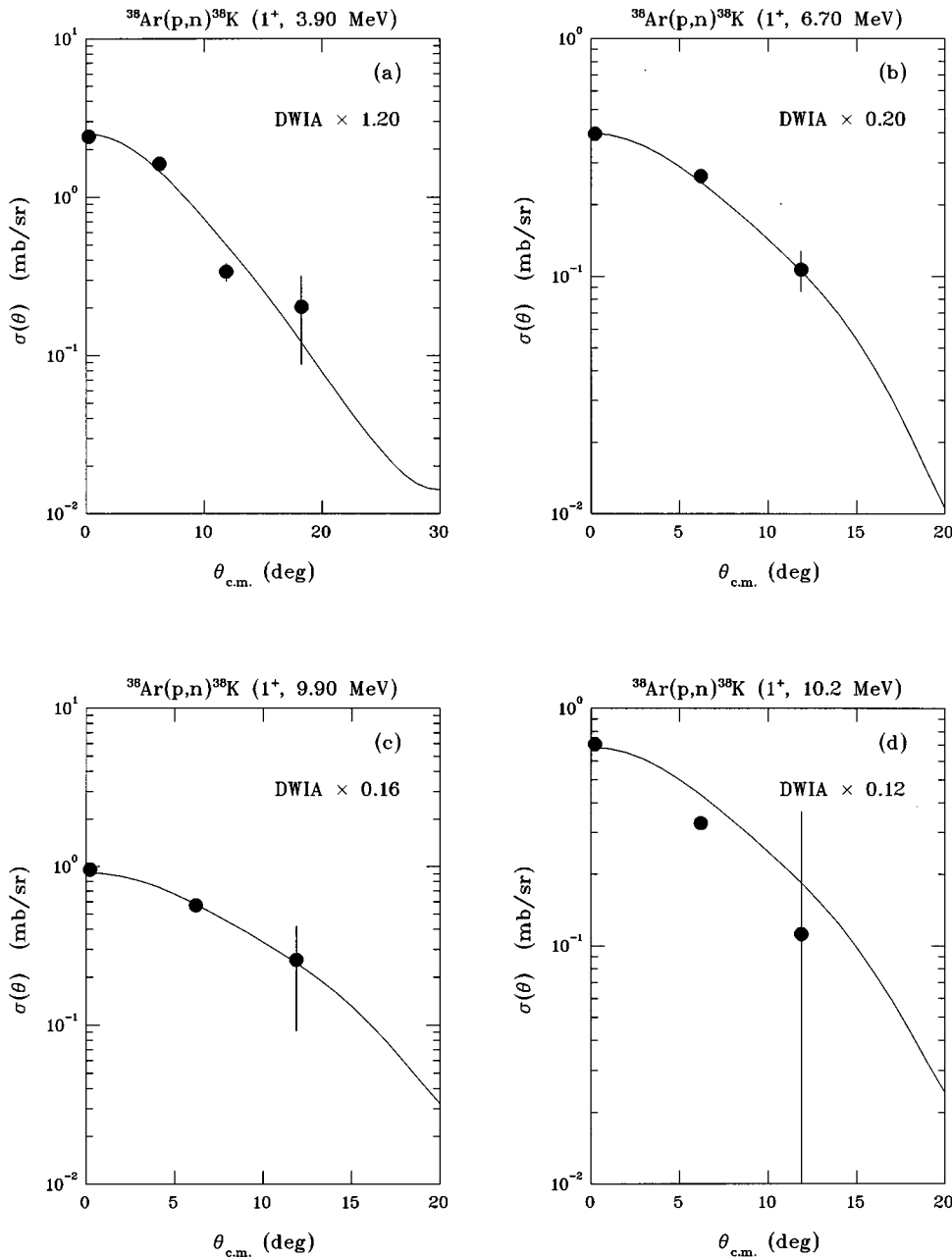FIG. 3. Angular distributions for the ^{38}Ar$(p,n)^{38}$K reaction at 135 MeV to the final states at 3.9, 6.7, 9.9, and 10.2 MeV.

3. The 1$^+$ state at 6.7 MeV

A weak peak is observed at 6.7 MeV. The angular distribution for this peak is shown in Fig. 3 and is peaked at 0°. Spin and parity assignments for levels above about 5 MeV in ^{38}K are unknown. The shell-model calculations predict a 1$^+$ state at 5.7 MeV and the DWIA calculation uses the wave function for this state. The calculations describe the angular distribution well with a normalization factor of 0.20.

4. The 1$^+$ states near 10 MeV

The last peak in Fig. 1 is a broad peak at about 10 MeV. In fitting this peak, we found it necessary to describe it with three individual peaks having widths consistent with those of the lower excitation-energy peaks. In Fig. 3 we show the angular distributions for the two strongest of these three peaks, viz., for the transitions to the states at 9.9 and 10.2

MeV. The distributions are clearly peaked at 0°. The shell-model calculations predict a $T=1$, 1$^+$ state at 8.8 MeV, and the DWIA calculations use the wave function for this state. The calculation agrees well with the forward-angle part of both angular distributions with normalization factors of 0.16 and 0.12, respectively.

III. THE ANALOG β-DECAY MEASUREMENT: ^{38}Ca$(\beta^+)^{38}$K

A. Experimental procedure

The β-decay experiment was performed at CERN with the on-line mass separator ISOLDE. Calcium isotopes were produced by bombarding a Ti target with the 1-GeV pulsed proton beam from the PS Booster. The proton pulses had a 2-μs width and a repetition rate of 1.2 s; the opening of the
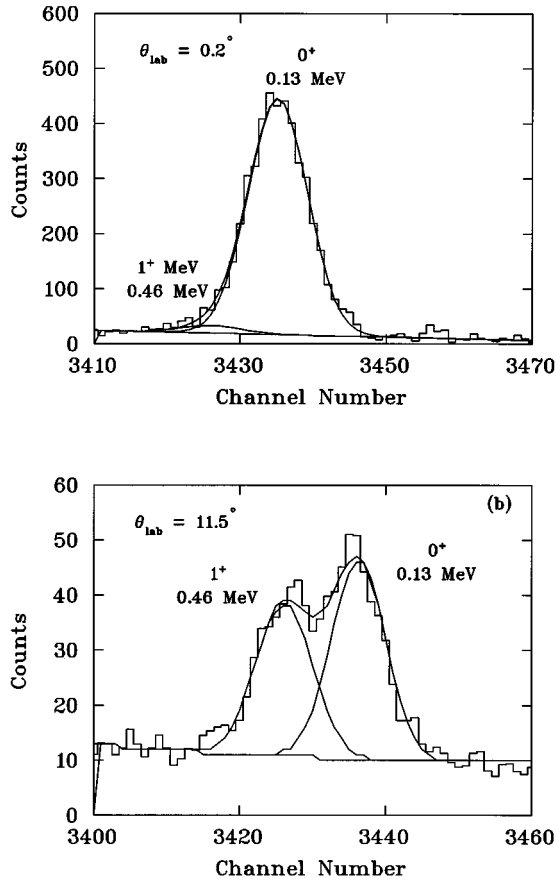
FIG. 4. Fits to the experimental time-of-flight spectra at 0.2° and 11.5° for the region of the 3^+, 0^+, 1^+ complex from 0.0 to 0.46 MeV of excitation.

FIG. 5. Gated spectrum of β-delayed γ rays from ^{38}Ca taken with the ^{38}Ca^{19}F$^+$ beam (log scale). All peaks (energies in keV) are assigned to the decay of ^{38}Ca. The strong peak at channel 2000 results from the sum $(1568 + 511)$ keV.

ISOLDE beam gate was delayed 10 ms with respect to the proton pulse and maintained for 500 ms to optimize the signal-background ratio. The different atoms were ionized through surface ionization and mass separated in the ISOLDE magnet. One major difficulty for the observation of weak lines in the ^{38}Ca(β^+)^{38}K decay [$T_{1/2}(^{38}$Ca$) = 440$ ms] is the strong activity of the isobars selected with the same magnetic field values: ^{38}K ($T_{1/2} = 7.64$ min) and ^{38}K^m ($T_{1/2} = 924$ ms). For the ^{38}K isotopes, higher production cross sections and better ionization efficiencies combine to give a yield, y, measured at the output of the separator several orders of magnitude higher than for Ca nuclides [^{38}K: $y = 10^8$ at/s, ^{38}K^m: $y = 10^6$ at/s, and for ^{38}Ca: $y = 10^4$ at/s]. In this case, in addition to the mass selectivity, a chemical selectivity was needed and could be found with the use of molecular sidebands [29]. The Ti rod target (93 g/cm^2), equipped with a W surface ionizer, was then operated with a CF$_4$ leak rate of 1.4×10^{-5} mbar l/s. The intensity of the CaF$^+$ beam, measured with the separator mass at $A = A$(Ca)$+19$, was found to amount to 30% of the beam of the corresponding elementary calcium ions. For $A = 57$, pure sources of ^{38}Ca were obtained as ^{38}Ca^{19}F$^+$, allowing for the first time the ^{38}Ca β decay to be investigated without contamination by isobars (as in previous separator experiments) or by other activities (as in rabbit-type experiments [30]). The CaF ion beam was directed onto the collecting zone of a
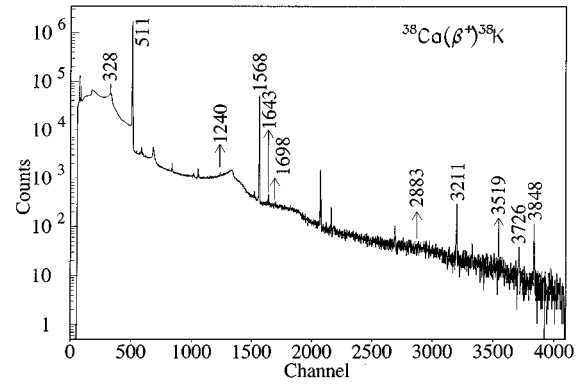
moving tape system. Daughter activity was periodically removed by driving the tape. The total number of ^{38}Ca ions collected during this experiment was 1.5×10^8. Special care is necessary to measure weak β transitions by looking for the corresponding γ-ray peaks. The setup was devised to optimize the γ detection efficiency and reject bremsstrahlung background or superposition of positrons and γ rays. The gamma spectrum was recorded with two Ge detectors (70% efficiency), operated in coincidence with positrons detected in a thin cylindrical plastic scintillator, surrounding the tape in a near 4π geometry. A thin flat plastic scintillator was placed in front of each Ge detector to avoid the simultaneous detection of positrons and gamma rays in the same counter. Events detected in a Ge diode were gated with the $4\pi\beta$ counter and vetoed when a positron was detected in the thin plastic in front of the same Ge detector. A passive shielding was installed between the gamma detectors and the various background activities.

B. β-decay: Results and discussion

The sum of all data collected with one Ge counter associated with the plastic scintillators corresponds to the spec-
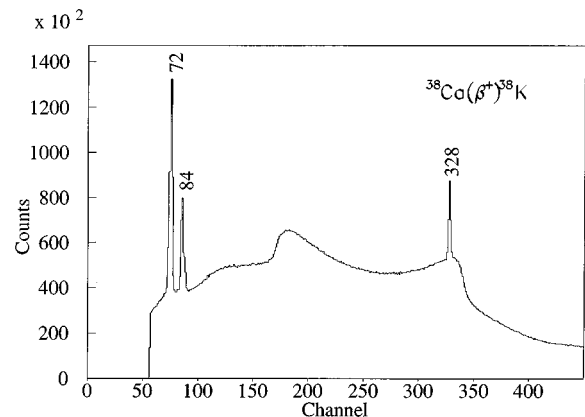

FIG. 6. Low-energy part of the gated γ-ray spectrum in linear scale. X rays result from absorption of positrons in the Pb shielding. The absence of contaminants and the presence of the 328-keV line, attributed to the decay of the 0.46 MeV level, can readily be seen.

TABLE I. Relative intensities of gamma transitions observed in this work.

E_γ (keV)	Transition		Relative intensities	
	E_i (keV)	E_f (keV)	This work	Ref. [30]
328	459	130	0.150(10)	0.126(16)
1240	1698	459	0.0024(5)	<0.010
1568	1698	130	1	1
1643	3342	1698	0.0040(5)	<0.010
1698	1698	0	0.0008(4)	<0.0082
2883	3342	459	0.007(2)	<0.0033
3211	3342	130	0.0138(10)	0.0139(15)
3519	3978	459	0.0004(3)	<0.0042
3716	4175	459	0.0002(1)	<0.0045
3726	3857	130	0.0019(2)	<0.0036
3848	3978	130	0.0056(5)	<0.0081

trum given in Fig. 5. No contaminants were observed in the molecular beam and all γ-ray peaks could be related to transitions between ^{38}K levels. The low-energy portion of the γ measurement is presented in Fig. 6. The γ transition of 328 keV, which corresponds to the β-decay transition to the 0.46-MeV level, appears close to the Compton edge ($E=341$ keV) of the scattering distribution resulting from the large number of 511-keV positron annihilation γ rays. This transition, not observed in the earliest measurements of ^{38}Ca(β^+)^{38}K [31–33], can be accurately measured in our experimental conditions.

Relative γ-ray efficiencies were measured with ^{56}Co and ^{152}Eu sources. Corrections were made for cascade summing in the ^{56}Co source measurement and for losses in the photopeak intensity resulting from summation between γ rays and 511-keV annihilation radiation in the ^{38}Ca β-decay experiment. For the superallowed Fermi branch [^{38}Ca(g.s., 0^+) $\rightarrow$ ^{38}K(130 keV, 0^+)], we have assumed a $\log ft$ value of 3.486, using the same conversion factor between model-independent Fermi strength and ft values as in the recent analyses of ^{36}Ca [13] and ^{37}Ca [34] decays. The relative γ intensities are given in Table I. The comparison of our results with the previous studies [30], where the ^{38}Ca activity was produced by the reaction ^{36}Ar(^{3}He,n)^{38}Ca, illustrates the gain in sensitivity obtained with the pure, mass-separated sources. In Table II are listed the absolute β branches and values of $\log ft$ derived from the measured relative γ-ray intensities. The proposed ^{38}Ca(β^+)^{38}K decay scheme is shown in Fig. 7. Three new β branches are reported, popu-

TABLE II. β-decay branching ratios and transition strengths observed in this work.

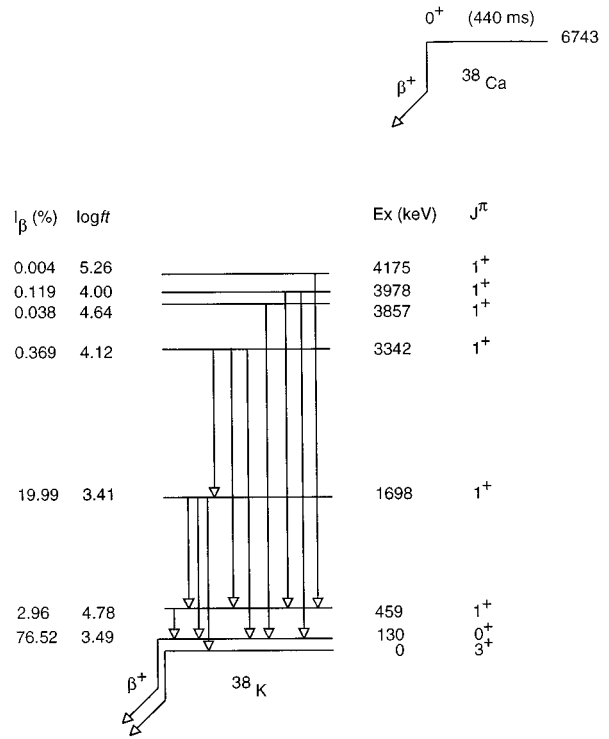| E_x (MeV)	J^π	I_β (%)	$\log ft$
0.130	0^+	76.52	3.49
0.459	1^+	2.96(15)	4.78(3)
1.698	1^+	19.99(30)	3.41(2)
3.342	1^+	0.369(13)	4.12(2)
3.857	1^+	0.038(4)	4.64(6)
3.978	1^+	0.119(8)	4.00(4)
4.175	1^+	0.004(2)	5.26(23)

FIG. 7. Proposed decay scheme for ^{38}Ca(β^+)^{38}K.

lating levels at 3857, 3978, and 4175 keV in ^{38}K. The nuclear properties of the two first ones were determined previously by transfer reactions with $J^\pi = 1^+$ assignments in both cases [35]. The 4175-keV level was previously reported [35] with $J^\pi = (1, 2)^+$. Our measurement ($\log ft = 5.26$) assigns $J^\pi = 1^+$ to this state. Furthermore, we have observed two γ rays, at 1643 and 2883 keV, which were tentatively assigned to new γ branches from the 3342 keV level (3342 keV, 1^+ to 1698 keV, 1^+ and 3342 keV, 1^+ to 459 keV, 1^+). Therefore, the intensity of the β branch to the 3342-keV level has been found to be stronger in our experiment than in previous work [30].

IV. GAMOW-TELLER STRENGTH

In order to compare the results of the (p,n) and β-decay measurements with each other, and also with the shell-model predictions, it is desirable to convert the β-decay ft values and the (p,n) cross sections to B(GT) values.

The transition strength in the β decay of ^{38}Ca is determined using the standard relationship between $\log ft$ value and B(GT) [36]:

$$B_\beta(\text{GT}) = K/ft,$$

where $K = 6127(9)$ s, as all branches to states above the isobaric analog state ($E_x = 0.130$ MeV) can be described as pure Gamow-Teller transitions. The corresponding B_β(GT) experimental values are reported in Table III. The unprecedented experimental conditions allow the determination of the GT distribution for six 1^+ states; the new β branches,

TABLE III. B(GT) values from the ^{38}Ar$(p,n)^{38}$K reaction, from ^{38}Ca$(\beta^+)^{38}$K β decay, and from a shell-model calculation (see text). The shell-model states at 5.42 and 8.78 MeV have $T=1$, all others have $T=0$.

(p,n)		β decay		Shell model			
E_x (pn) (MeV)	B_{pn}(GT)	$E_x(\beta)$ (MeV)	B_β(GT)	E_x(SM) (MeV)	$B_{\text{free}}^{\text{SM}}$(GT)	B_β^{SM}(GT)	B_{pn}^{SM}(GT)
0.46	0.010(5)	0.459	0.064(4)	0.13	0.559	0.260	0.115
1.70	1.73(25)	1.698	1.48(4)	1.71	3.354	1.774	2.094
3.4	0.23(4)	3.342	0.29(3)				
		3.857	0.088(10)	3.73	0.418	0.226	0.212
3.9	0.43(7)	3.978	0.372(25)				
		4.174	0.021(10)				
				5.42	0.000	0.000	0.007
6.7	0.07(2)			5.62	0.405	0.197	0.163
9.7	0.03(1)						
9.9	0.17(3)			8.78	1.252	0.633	0.562
10.2	0.13(2)						
				14.6	0.010	0.003	0.002
Σ B(GT) $=$	2.93(44)		2.416(24)		6.000	3.094	3.155

observed in this study, amount to only 0.16% of the total decay but correspond to 21% of the total B(GT) strength in the β window.

In order to convert the (p,n) cross sections to B(GT) strength, we use a ''universal'' conversion factor determined previously by comparing 0° (p,n) cross sections with analog B(GT) values from β decay for several $1s0d$-shell nuclei [4]. For the reaction of interest here, we can check this conversion factor because the β-decay analog of the transition to the strongly excited state at 1.7 MeV has been observed and the B(GT) value determined.

Following the method of Ref. [4], we have

$$B_{pn}(\text{GT})=0.064\frac{\sigma(q=0)}{N_D},$$

where $\sigma(q=0)$ is the (p,n) cross section extrapolated to zero-momentum transfer, and

$$N_D=\frac{\sigma_{\text{DW}}(0°)}{\sigma_{\text{PW}}(0°)}$$

is the distortion factor, calculated as the ratio of the DWIA-calculated cross sections with and without distortion. The factor of 0.064 is the ''universal'' conversion factor obtained previously. (Note that this factor is expected to be energy dependent, but was determined for 135 MeV, the energy of this experiment.) For this reaction, the ratio of the cross sections extrapolated to zero-momentum transfer to the 0° cross sections is about 1.05 (estimated from DWIA calculations), and the distortion factor is 0.38. The result is that the net conversion factor for this reaction is

$$B_{pn}(\text{GT})=0.177\sigma_{pn}(0°).$$

The resulting B_{pn}(GT) values are listed in Table III. The B(GT) units are such that the B(GT) value for the β decay of the free neutron is 3.0. The uncertainties are indicated in parentheses and are the quadratic combination of the system-

atic uncertainty of 12%, as discussed in Sec. II, plus the fitting uncertainties for each complex. In general, the systematic uncertainty dominates, except for the weak 0.46-MeV transition where the fitting uncertainty was large because the state could not be separated completely from the stronger transition to the 0^+, IAS at 0.13 MeV (see discussion above).

The B_{pn}(GT) values are compared with the B_β(GT) values in Table III. As indicated, the agreement of the β-decay B(GT) values with those from the (p,n) reaction is reasonably good. For the strong transition to the state at 1.7 MeV, the (p,n) result is 17% larger than the β-decay result. The earlier β-decay measurement of Wilson et al. [30] obtained B(GT) = 1.583, which is within 10% of the (p,n) result. Besides the very strong transition at 1.7 MeV, both the (p,n) and β-decay B(GT) distributions indicate a B(GT) strength of about 0.25 at 3.4 MeV, and about 0.45 at 3.9 MeV. The β-decay measurements reveal two weakly excited states near the strongly excited state at 3.9 MeV, which are unresolved from the strong transition in the (p,n) measurements. The only significant difference between the two experiments is for the ''ℓ-forbidden'' transition to the state at 0.46 MeV, for which the (p,n) result of 0.010 is significantly smaller than the β-decay result of 0.064. As we will discuss below, the difference observed for the strong state at 1.7 MeV as well as the large difference observed for this very weak state can be explained by the difference between the effective operators for the β decay and the (p,n) reaction.

It is significant that the (p,n) measurements show some strength at higher excitation energies, above the β-decay Q-value window, viz., near 7 and 10 MeV of excitation; however, we note that this strength is relatively weak, amounting to only 16% of the strength observed at lower excitation energies. The strength predicted at 8.8 MeV is to a 1^+ $T=1$ state (all of the other calculated strength in Table III is to $T=0$ states). Essentially all of the theoretical strength to $T=1$ states is concentrated in this single state. In
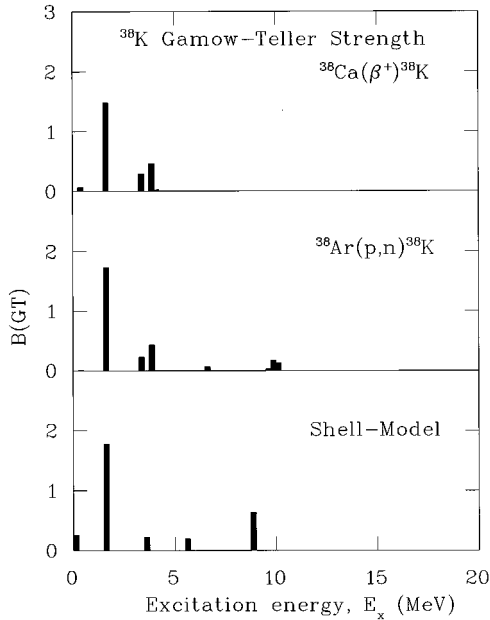
FIG. 8. Comparison of the experimental B_{pn}(GT) and B_β(GT) spectra with the CWH shell-model predictions. The theoretical spectrum was calculated using "effective" GT operators (see text).

Ref. [37], the $M1$ transitions to the analogs of the 1^+ $T=1$ states in ^{38}Ar were studied by inelastic electron scattering. In that study it was found that the $M1$ strength was fragmented over many states in the $7-14$ MeV excitation-energy range; this is understood as a fragmentation of the simple 0p-2h configuration over many (2p-4h) configurations. Thus it is likely that much of the predicted strength to 1^+ $T=1$ states is located in small peaks that we cannot separate from the continuum background. The total strength to $T=0$ states is 2.63, compared to the calculated free-nucleon value of 4.75. This result is consistent with that observed for other $1s0d$-shell nuclei and indicates "quenching" for this case.

Table III also presents the B(GT) values predicted by the CWH shell-model calculation described above. B(GT) values were obtained from the one-body transition densities (OBTD's) using both "free-nucleon" and "effective" GT matrix operators [2]. The "effective" GT operators were obtained by fitting to available β-decay GT transitions in the $1s0d$ shell [2]. As seen, the total GT strength predicted by the free-nucleon operator calculations necessarily satisfies the $3(N-Z)$ sum rule, although these calculations overestimate the experimental results by a factor of about 2. The predictions obtained using the "effective" GT operators are in much better agreement with experiment. The shell-model GT spectrum using the "effective" operators is compared with the β decay and (p,n) B(GT) values in Fig. 8. One sees that the distribution of GT strength is reasonably well predicted by the shell-model calculation. This calculation predicts that the majority of the GT strength should appear in a single state at 1.7 MeV, with less strength distributed up to about 10 MeV. This result is in good agreement with the experimental results from both the β decay and (p,n) measurements. The fragmentation of the strength differs somewhat from the CWH shell-model prediction if we take into

account the weakly excited states revealed by the β probe. Five 1^+ states are observed below 4 MeV while the calculation predicts only three states in this energy range. The additional experimental 1^+ levels seem to be related to configurations outside the $1s0d$-model space. Calculations in the full sd-fp space are not achievable, but a shell-model estimate obtained in a $d_{3/2}$-$f_{7/2}$ space reveals an intruder 1^+ state coming in at 3.2 MeV with a small B(GT) value, in agreement with the experiment. More 1^+ levels are predicted below 13 MeV but with extremely small strength [B(GT) $= (2-5)\times10^{-3}$]. Intruder state mixing into the final states has the effect of spreading the local GT strength, but does not change the total strength. Intruder state mixing into the initial ground state can also redistribute the strength between β^+ and β^- and between low (the $1s0d$ shell part below about 15 MeV) and high (many $\hbar\omega$) excitation energy, and it is this higher-order configuration mixing which gives rise to at least part of the quenching [38,39].

As noted above, there are some differences between the β-decay results and the (p,n) results, especially for the first 1^+ state at 0.46 MeV where the B(GT) value obtained from the β-decay measurements are $\sim6\times$ larger than the value obtained from the (p,n) measurement. As can be seen in Fig. 2, the (p,n) angular distribution is not peaked at 0° as expected for a $\Delta\ell = 0$, GT transition. In Ref. [14] we suggested an empirical modification to the effective GT operator for (p,n) reactions, which enhanced the ℓ-forbidden part of the GT$_{pn}$ operator compared to the value needed for the GT$_\beta$ operator. The 1^+ state at 0.46 MeV is an ideal candidate to test this effective operator. In Table III we give the B_{pn}(GT) values calculated with the effective GT$_{pn}$ operator. The calculated B_{pn}(GT) value for the lowest 1^+ state is over a factor of 2 smaller than B_β(GT) in the direction observed in experiment. This large reduction relative to B_β(GT) is due to a destructive interference between the allowed spin operator and the (enhanced) ℓ-forbidden operator. For the strong state at 1.7 MeV the spin and ℓ-forbidden contributions are in phase leading to an 18% increase in B_{pn}(GT) relative to B_β(GT), again in agreement with experiment.

The calculation for the lowest 1^+ state can perhaps be made more realistic by mixing the first and second shell-model 1^+ states to reproduce the observed B_β(GT) value of 0.064 exactly (with the effective GT$_\beta$ operator of Ref. [2]). The mixed wave function is $|1^+,\text{mixed}\rangle = 0.982|1_1^+\rangle + 0.189|1_2^+\rangle$. Then with the same mixed wave function we switch the operator to GT$_{pn}$ and obtain B_{pn}(GT) $= 0.005$, in good agreement with experiment. With the mixed wave function, there is almost an exact cancellation between the spin ℓ-forbidden contributions to (p,n). When the empirical (p,n) operator was first introduced [14], it was used to explain cases where the B_{pn}(GT) was enhanced relative to B_β(GT) (such as the $A=15$ g.s. to g.s. and $A=39$ g.s. to g.s., GT transitions). Here we find an example where the enhanced ℓ-forbidden operator makes B_{pn}(GT) much smaller than B_β(GT). The effective GT$_{pn}$ operator was used recently to set limits on the ^{71}Ga GT strength, which is important for solar neutrino experiments [40]. It would be important in the ^{71}Ga case to determine whether there is constructive or destructive interference between the spin and ℓ-forbidden

terms. A destructive interference would presumably be characterized by an angular distribution that is not peaked at 0°.

We note that the β-decay transition to the 0.46-MeV level was not observed in the earliest measurements of ^{38}Ca(β^+)^{38}K [31–33], although it was observed in the more recent measurements of Wilson *et al.* [30] and in the present work. The β-decay branching ratio is determined by measuring the delayed γ rays emitted by the decays of excited states of ^{38}K. The γ decays of the 1^+ (GT) states are primarily to the 0^+, IAS state at 0.13 MeV. The difficulty in observing the transition to the 0.46-MeV state was that its decay yields a 328-keV γ ray appearing only as a small peak on the Compton edge of the 511-keV positron annihilation γ rays that are present (see the discussion in Wilson *et al.* [30]).

In any event, we are confident of our analyses here for this transition in both the (p,n) and β-decay (see Fig. 6) experiments with the uncertainties quoted. Certainly this case provides a difference between (p,n) and β decay that is puzzling. This difference is the largest known among numerous comparisons between (p,n) and analog β decays for "allowed" GT transitions from even-even target nuclei. We have observed other cases of 0^+ to 1^+ transitions that have (p,n) angular distributions not peaked at 0°, e.g., the ^{32}S(p,n)^{32}Cl(g.s.) transition [15]. In this case, the very small B(GT) values observed from the ^{32}P and ^{32}Cl β decay, B(GT) = 0.000 14 and 0.0021, respectively [2], indicate the near vanishing of the spin matrix element—in agreement with the sd-shell calculations [2]. There is a sizable $s_{1/2}-d_{3/2}$ ℓ-forbidden component to this transition, which leads to B_{pn} = 0.0083 (with the effective pn operator) in agreement with the value of 0.009(5) extracted from the (p,n) experiment [15]. In contrast, the effect for the present $A=38$ case is much more dramatic because of the destructive interference between spin and ℓ-forbidden components which are about the same size.

V. CONCLUSIONS

We studied the distribution of Gamow-Teller (GT) strength in the ^{38}Ar(p,n)^{38}K reaction at 135 MeV and the analog β-decay ^{38}Ca(β^+)^{38}K reaction. For the (p,n) reaction, transitions with $\Delta\ell = 0$ angular distributions were identified and the 0° cross sections were converted to

B_{pn}(GT) values using a "universal" conversion factor, which was obtained by comparing (p,n) cross sections with B(GT) values for other analog β decays in the $1s0d$ shell. In this work, analog B(GT) values were obtained from the β-decay experiment where pure Ca sources and efficient β-γ measurements allowed a sensitivity around 4×10^{-5} for the population of 1^+ states. The (p,n) and the β-decay results are consistent, except for the transition to the first 1^+ state at 0.46 MeV. The (p,n) measurements extend the β-decay measurements because the (p,n) reaction has no kinematic cutoff. The difference observed for the 0.46-MeV transition is significant; the (p,n) result is $\sim6\times$ smaller than the β-decay result. This difference can be accounted for by using separate "effective" (p,n) and β-decay GT operators obtained earlier.

The summed B_{pn}(GT) strength is less than 50% of the simple Ikeda sum rule for this reaction, consistent with the results obtained for several other $1s0d$-shell nuclei. The summed B_β(GT) strength in this favorable case amounts to 80% of the total experimental strength, corresponding to the summed B_{pn}(GT). The summed B_β(GT) is in excellent agreement with the $1s0d$ shell-model calculation of the strength in the β-decay "window" using "effective" GT matrix operators. In the total range probed with the (p,n) reaction, the distribution of GT strength is reproduced well by this shell-model evaluation. The shell-model calculation uses the same basis and matrix elements as one employed recently by Brown [12] to describe successfully the GT distribution in $A=37$. For this case, as for several other $1s0d$-shell nuclei, we conclude that there does appear to be "missing" GT strength, which indicates the need for renormalization of the GT operator used for comparison of the shell-model calculations and the Ikeda sum rule to the strength observed in low-lying states.

[1] B.A. Brown, W. Chung, and B.H. Wildenthal, Phys. Rev. Lett. **40**, 1631 (1978); B.A. Brown and B.H. Wildenthal, Phys. Rev. C **28**, 2397 (1983).

[2] B.A. Brown and B.H. Wildenthal, Atom. Data Nucl. Data Tables **33**, 347 (1985).

[3] R. Madey, B.S. Flanders, B.D. Anderson, A.R. Baldwin, C. Lebo, J.W. Watson, S.M. Austin, A. Galonsky, B.H. Wildenthal, and C.C. Foster, Phys. Rev. C **35**, 2011 (1987).

[4] B.D. Anderson, T. Chittrakarn, A.R. Baldwin, C. Lebo, R. Madey, P.C. Tandy, J.W. Watson, C.C. Foster, B.A. Brown, and B.H. Wildenthal, Phys. Rev. C **36**, 2195 (1987).

[5] B.D. Anderson, N. Tamimi, A.R. Baldwin, M. Elaasar, R. Madey, D.M. Manley, M. Mostajabodda'vati, J.W. Watson, W.M. Zhang, and C.C. Foster, Phys. Rev. C **43**, 50 (1991).

[6] A. Willis, M. Morlet, N. Marty, C. Djalali, G.M. Crawley, A. Galonsky, V. Rotberg, and B.A. Brown, Nucl. Phys. **A464**, 315 (1987).

[7] G.M. Crawley, C. Djalali, N. Marty, M. Morlet, A. Willis, N. Anantaraman, B.A. Brown, and A. Galonsky, Phys. Rev. C **39**, 311 (1989).

[8] N. Marty, in *Weak and Electromagnetic Interactions in Nuclei*, edited by H.V. Klapdor (Springer-Verlag, Berlin, 1986), p. 268.

[9] K.I. Ikeda, S. Fujii, and J.I. Fujita, Phys. Lett. **3**, 271 (1963).

[10] E.G. Adelberger, A. Garcia, P.V. Magnus, and D.P. Wells, Phys. Rev. Lett. **67**, 3658 (1991).

[11] D.H. Wilkinson, Nucl. Phys. **A225**, 365 (1974).

[12] B.A. Brown, Phys. Rev. Lett. **69**, 1034 (1992).

[13] W. Trinder, E.G. Adelberger, B.A. Brown, Z. Janas, H. Keller, K. Krumbholz, V. Kunze, P. Magnus, F. Meissner, A. Piechaczek, M. Pfützner, E. Roeckl, K. Rykaczewski, W.-D. Schmidt-Ott, and M. Weber, Phys. Lett. B **348**, 331 (1995).

[14] J.W. Watson, W. Pairsuwan, B.D. Anderson, A.R. Baldwin, B.S. Flanders, R. Madey, R.J. McCarthy, B.A. Brown, B.H. Wildenthal, and C.C. Foster, Phys. Rev. Lett. **55**, 1369 (1985).

[15] B.D. Anderson, T. Chittrakarn, A.R. Baldwin, C. Lebo, R. Madey, R.J. McCarthy, J.W. Watson, B.A. Brown, and C.C. Foster, Phys. Rev. C **31**, 1147 (1985).

[16] B.D. Anderson, C. Lebo, A.R. Baldwin, T. Chrittrakarn, R. Madey, J.W. Watson, and C.C. Foster, Phys. Rev. C **41**, 1474 (1990).

[17] A.R. Baldwin and R. Madey, Nucl. Instrum. Methods **171**, 149 (1980).

[18] R. Madey *et al.*, Nucl. Instrum. Methods **214**, 401 (1983).

[19] P.R. Bevington, *Data Reduction and Error Analysis for the Physical Sciences* (McGraw-Hill, New York, 1969), p. 237.

[20] R. Cecil, B.D. Anderson, and R. Madey, Nucl. Instrum. Methods **161**, 439 (1979).

[21] J.W. Watson, B.D. Anderson, A.R. Baldwin, C. Lebo, B. Flanders, W. Pairsuwan, R. Madey, and C.C. Foster, Nucl. Instrum. Methods **215**, 413 (1983).

[22] J. D'Auria, M. Dombsky, L. Moritz, T. Ruth, G. Sheffer, T.E. Ward, C.C. Foster, J.W. Watson, B.D. Anderson, and J. Rapaport, Phys. Rev. C **30**, 1999 (1984).

[23] Program DWBA70, R. Schaeffer and J. Raynal (unpublished); J.R. Comfort, Extended version DW81 (unpublished).

[24] M.A. Franey and W.G. Love, Phys. Rev. C **31**, 488 (1985).

[25] P. Schwandt, H.O. Meyer, W.W. Jacobs, A.D. Bacher, S.E. Vigdor, M.D. Kaitchuck, and T.R. Donoghue, Phys. Rev. C **26**, 55 (1982).

[26] B.A. Brown, A. Etchegoyen, W.D.M. Rae, and N.S. Godwin, Computer code OXBASH (unpublished).

[27] B.D. Anderson, M. Mostajabodda'vati, C. Lebo, R.J. McCarthy, L. Garcia, J.W. Watson, and R. Madey, Phys. Rev. C **43**, 1630 (1991).

[28] *Table of Isotopes*, edited by C.M. Lederer and V.S. Shirley, 7th ed. (Wiley, New York, 1978).

[29] E. Hagebø, P. Hoff, O. C. Jonsson, E. Kugler, J. P. Omtvedt, H. L. Ravn, and K. Steffensen, Nucl. Instrum. Methods B **70**, 165 (1992).

[30] H.S. Wilson, R.W. Kavanagh, and F.M. Mann, Phys. Rev. C **22**, 1696 (1980).

[31] J.E. Cline and P.R. Chagnon, Phys. Rev. **108**, 1495 (1957).

[32] R.W. Kavanagh, A. Gallmann, E. Aslanides, F. Jundt, and E. Jacobs, Phys. Rev. **175**, 1426 (1968).

[33] A. Gallmann, E. Aslanides, F. Jundt, and E. Jacobs, Phys. Rev. **186**, 1160 (1969).

[34] W. Trinder, E. G. Adelberger, Z. Janas, H. Keller, K. Krumbholz, V. Kunze, P. Magnus, F. Meissner, A. Piechaczek, M. Pfützner, E. Roeckl, K. Rykaczewski, W. D. Schmidt-Ott, and M. Weber, Phys. Lett. B **349**, 267 (1995).

[35] P. M. Endt, Nucl. Phys. **A521**, 1 (1990).

[36] D. H. Wilkinson, Nucl. Instrum. Methods. A **335**, 172 (1993); **335**, 201 (1993).

[37] C.W. Foltz, D.I. Sober, L.W. Fagg, H.D. Gräf, A. Richter, E. Spamer, and B.A.Brown, Phys. Rev. C **49**, 1359 (1994).

[38] B. A. Brown and B. H. Wildenthal, Nucl. Phys. **A474**, 290 (1987).

[39] A. Arima, K. Schimizu, W. Bentz, and H. Hyuga, Adv. Nucl. Phys. **18**, 1 (1987); I. S. Towner, Phys. Rep. **155**, 264 (1987).

[40] N. Hata and W.C. Haxton, Phys. Lett. B **353**, 422 (1995).